


RESEARCH ARTICLE

Effect of increased ocean resolution on model errors in El Niño–Southern Oscillation and its teleconnections

Ned C. Williams¹  | Adam A. Scaife^{1,2} | James A. Screen¹¹Faculty of Environment, Science and Economy, University of Exeter, Exeter, UK²Met Office Hadley Centre, Exeter, UK**Correspondence**

Ned C. Williams, Faculty of Environment, Science and Economy, University of Exeter, Exeter, UK.

Email: nw432@exeter.ac.uk**Funding information**

Natural Environment Research Council, Grant/Award Number: NE/L002434/1; Department for Business, Energy and Industrial Strategy, UK Government

Abstract

Despite the complexity of the underlying processes, coupled climate models simulate fairly realistic El Niño–Southern Oscillation dynamics and teleconnections. However, there are many long-standing errors that remain. We use the High Resolution Model Intercomparison Project suite of models to assess how El Niño–Southern Oscillation and its late-winter teleconnection to the North Pacific changes when ocean resolution is quadrupled from 1° to 0.25°. We find that increased resolution eliminates large errors in the western extent of El Niño and La Niña sea-surface temperature anomalies, and that there is some improvement in the asymmetry between El Niño and La Niña. In low-resolution models, the teleconnections from El Niño and La Niña to the North Pacific are both underestimated and are centred too far west. With increased resolution, the position of the teleconnection is highly accurate during El Niño, but there is less improvement during La Niña. We find no significant improvements in teleconnection strength for either phase. Tropical mean-state sea-surface temperatures are found to be too cold by around 1°C throughout the central/eastern Pacific in low-resolution models, but this bias is not present in high-resolution models. Despite this, a large discrepancy between observed and modelled mean-state tropical rainfall persists in high-resolution models, which may limit improvements in the simulation of the La Niña teleconnection.

KEYWORDS

ENSO, HighResMIP, teleconnections

1 | INTRODUCTION

El Niño–Southern Oscillation (ENSO) teleconnections are the single largest source of variability and predictability on seasonal time-scales. Accurate modelling of ENSO and its teleconnections is therefore crucial for long-range forecasting. Despite continued improvement, differences between observed and modelled ENSO events and their

teleconnections still occur due to model errors. Future ENSO characteristics beyond an expected increase in associated rainfall anomalies under greenhouse-gas-induced warming are poorly understood due to a lack of model consensus (Cai et al., 2020).

The simplest picture of ENSO describes the fluctuation of sea-surface temperatures (SSTs) in the eastern and central tropical Pacific, between a warmer (El Niño) and

cooler (La Niña) phase. ENSO is not a symmetric phenomenon, however, with El Niño events typically being stronger and further east than La Niña events (Burgers & Stephenson, 1999), as well as having a shorter duration (Larkin & Harrison, 2002; Okumura & Deser, 2010). Strong El Niño events tend to involve strong SST anomalies in the far east of the tropical Pacific, whereas east Pacific SST anomalies are usually small during La Niña and moderate El Niño events (Deser & Wallace, 1987).

SST anomalies lead to changes in precipitation, and this relationship is nonlinear with a strong dependence on mean-state temperatures, resulting in a higher sensitivity to SST anomalies in the warmer western tropical Pacific than the east of the basin. Consequently, the strongest precipitation anomalies are found west of the strongest SST anomalies (Deser & Wallace, 1990). Precipitation exhibits a strong correlation with divergence at the level of convective outflow, leading to anomalous divergent wind in the Tropics and Subtropics. Overlap with the subtropical jet results in an anomalous source of Rossby waves, which then propagate to the extratropics (Sardeshmukh & Hoskins, 1988).

The extratropical North Pacific response to El Niño in winter is characterised by an equivalent barotropic deepening of the Aleutian low, and an approximately reversed response exists during La Niña. This leads to an anticyclonic anomaly (cyclonic during La Niña) over northern North America (Horel & Wallace, 1981). This Rossby wave-train response, known as the Pacific–North American pattern, is highly robust and affects temperature and precipitation on seasonal time-scales over North America. It is strongest during late winter (January–March, JFM), and so we focus on that period in this study. During El Niño, the wave train often continues to the North Atlantic and projects onto the negative phase of the North Atlantic Oscillation during late winter and onto the positive phase during early winter, with an opposite response during La Niña (Ayarzagüena et al., 2018; Moron & Gouirand, 2003). The North Atlantic response is also modulated by the stratosphere (Cagnazzo & Manzini, 2009; Ineson & Scaife, 2009) and, in particular during strong El Niño events, the tropical Atlantic (Toniazzo & Scaife, 2006).

Various systematic model errors relevant to ENSO and the generation and propagation of its teleconnections exist in current models. The east Pacific “cold tongue” is often too cold in models (Li & Xie, 2014), and models typically exhibit the “double intertropical convergence zone” phenomenon, whereby the observed zonal band of precipitation known as the intertropical convergence zone is too far north, a second band forms below the Equator, and precipitation on the Equator itself is underestimated (Lin, 2007). The observed asymmetry of the distribution

of eastern Pacific SST anomalies is also not generally captured by models (Ineson et al., 2021; Zhang & Sun, 2014). This affects the simulation of impacts due to strong El Niño events, as well as whether the model produces such events at all. Underestimated ENSO asymmetry has been linked to model disagreement on how future climate change may affect ENSO (Hayashi et al., 2020). Positive SST anomalies associated with El Niño (and negative anomalies associated with La Niña) tend to extend further westward in models than in observations (Luo et al., 2005). Accurate representation of teleconnections is potentially hindered by an underestimated sensitivity of tropical precipitation to local SST anomalies (Good et al., 2021). Errors in the modelling of extratropical processes may also be relevant to ENSO teleconnections, including underestimation of eddy feedback (Hardiman et al., 2022; Kang et al., 2011), or an atmospheric mean state that is unfavourable to observed Rossby wave propagation (Dawson et al., 2011; Li et al., 2020). Teleconnections from ENSO to the North Pacific are underestimated in seasonal forecast models, with a primarily extratropical source of the problem during El Niño (Williams et al., 2023). A similar error has also been found in subseasonal forecasts (Garfinkel et al., 2022).

The High Resolution Model Intercomparison Project (HighResMIP; Haarsma et al., 2016) is part of phase 6 of the Coupled Model Intercomparison Project and includes at least two different model versions from each contributing centre, with differing ocean and/or atmosphere resolutions. Liu et al. (2022) use HighResMIP to assess the impact of increased oceanic and atmospheric resolution on a variety of metrics associated with ENSO. In particular, they find increasing ocean resolution reduces model biases in the equatorial Pacific SST mean state. They also find increased (and hence improved) skewness in the Niño 3.4 region with increased ocean resolution, although previous studies (e.g., Burgers & Stephenson, 1999) have found the asymmetry to be small in this region compared with other regions of the tropical Pacific. Both Liu et al. (2022) and Moreno-Chamarro et al. (2022) find improvement in mean-state tropical Pacific precipitation with increased ocean resolution in HighResMIP models, although both find that this improvement is weaker than expected given the improvement in mean-state SSTs.

Here, we use HighResMIP simulations to understand the effect of increasing horizontal ocean resolution from 1° to 0.25° on ENSO during winter (December–March, DJFM), as well as the resulting impact on teleconnections to the extratropical North Pacific during late winter (JFM). We first assess the capability of low and high ocean-resolution models to capture the spatial pattern and asymmetry of boreal winter tropical SST anomalies during El Niño and La Niña. We then examine the impact

TABLE 1 The models used in this study, with the developing centre, ocean grid, classification as low resolution (LR) or high resolution (HR), and number of ensemble members.

Model	Centre	Ocean grid	LR/HR	Atmos. res. (km) ^a	Members
CNRM-CM6.1	CNRM-CERFACS	ORCA1	LR	156	1
EC-Earth-3P	EC-Earth-Consortium	ORCA1	LR	78	3
ECMWF-IFS-LR	ECMWF	ORCA1	LR	50	8
HadGEM3-GC3.1-LL	MOHC	ORCA1	LR	208	6
CNRM-CM6.1-HR	CNRM-CERFACS	ORCA025	HR	55	1
CMCC-CM2-HR4	CMCC	ORCA025	HR	139	1
CMCC-CM2-VHR4	CMCC	ORCA025	HR	35	1
EC-Earth-3P-HR	EC-Earth-Consortium	ORCA025	HR	39	3
ECMWF-IFS-MR	ECMWF	ORCA025	HR	50	3
ECMWF-IFS-HR	ECMWF	ORCA025	HR	25	6
HadGEM3-GC3.1-MM	MOHC	ORCA025	HR	93	3
HadGEM3-GC3.1-HM	MOHC	ORCA025	HR	39	1
HadGEM3-GC3.1-HH	MOHC	ORCA12	HR	39	1

Abbreviations: CMCC, Centro Euro-Mediterraneo sui Cambiamenti Climatici; CNRM-CERFACS, Centre National de Recherches Météorologiques and Centre Européen de Recherche et Formation Avancée en Calcul Scientifique; ECMWF, European Centre for Medium-Range Weather Forecasts; MOHC, Met Office Hadley Centre.

^a Atmospheric resolution at 0°N.

that this has on the North Pacific circulation response to both ENSO phases. Finally, we try to understand how the changes in teleconnections arise from the increase in ocean resolution.

2 | METHODOLOGY

We consider 13 HighResMIP models, listed in Table 1. All 13 models use NEMO (Madec et al., 2017) for the ocean component; this allows us to reduce model-dependent variation in ocean simulation, while still considering almost all models within HighResMIP. Four models (CNRM-CM6.1, EC-Earth-3P, ECMWF-IFS-LR, and HadGEM3-GC3.1-LL) use the ORCA1 ocean grid, with a zonal resolution of 1° and a meridional resolution of 1/3° in the Tropics (15°S–15°N; 1° elsewhere) and are classed as low resolution (hereafter LR). Eight models (CMCC-CM2-HR4, CMCC-CM2-VHR4, CNRM-CM6.1-HR, EC-Earth-3P-HR, ECMWF-IFS-MR, ECMWF-IFS-HR, HadGEM3-GC3.1-MM, and HadGEM3-GC3.1-HM) use the ORCA025 grid with a 0.25° resolution and are classed as high resolution (HR). Additionally, the HadGEM3-GC3.1-HH model uses a 1/12° ocean grid (ORCA12) and is included as part of HR. We use the “hist-1950” set of HighResMIP simulations, which are run with observed greenhouse gas forcing over the period 1950–2014. The number of ensemble members per model

varies (see Table 1), but the HR and LR ensembles both consist of 20 members each. All variables are linearly detrended. Atmospheric resolutions are given in Table 1; although the atmospheric resolution is higher on average in the HR ensemble, there is considerable spread in both ensembles with significant overlap.

We compare tropical SST statistics with those from the HadISST dataset (Titchner and Rayner 2014; Kennedy et al. 2017 for the version used in this study). Atmospheric fields are compared with the Japanese 55-year Reanalysis (JRA-55; Kobayashi et al., 2015) from 1979/80 to 2019/20. For most variables, we use JFM means, as the teleconnection to the North Pacific is strongest in this period. We use DJFM for SSTs, as ENSO is partially phase locked to the early part of this period (Li, 1997; Rasmusson & Carpenter, 1982). We classify seasons as El Niño if the Niño 3.4 anomaly ($\Delta N_{3.4}$) is greater than 0.5 K, as La Niña if $\Delta N_{3.4}$ is less than -0.5 K, and neutral otherwise ($|\Delta N_{3.4}| < 0.5$ K). We find that using a threshold of ± 1 K instead does not qualitatively change the results. We compute El Niño and La Niña responses using composites of the relevant phase with the neutral composite subtracted. We quantify the westward extent of positive SST anomalies in the Pacific during El Niño—and negative anomalies during La Niña—using the point where equatorial SST anomalies are zero. To do this, we consider equatorial grid points between 120 and 200°E and interpolate between the easternmost set of adjacent points with opposing signs.

We measure ENSO SST asymmetry using skewness, defined for a sample as

$$\text{Skewness} = \frac{m_3}{(m_2)^{3/2}}, \quad (1)$$

where m_k is the k th central moment:

$$m_k = \sum_{i=1}^N \frac{(x_i - \bar{x})^k}{N}, \quad (2)$$

with x_i representing each realisation, \bar{x} the sample mean, and N the sample size. This metric of ENSO asymmetry has been used in various previous studies, starting with Burgers and Stephenson (1999). Skewness can be thought of as the non-normality of the sample distribution. When calculating skewness of multimodel distributions, we remove the mean of the individual model from each realisation.

To calculate the position of the North Pacific geopotential height response, we consider only points between 150 and 240°E and north of 20°N. We then restrict to grid points with a negative response during El Niño, or a positive response during La Niña, and then further restrict to points where the magnitude of the response is over half of the maximum. The longitude of the response λ_{NP} is computed as the response-weighted mean longitude of the points considered:

$$\lambda_{\text{NP}} = \frac{\sum_{N_y} \sum_{N_x} \lambda \Delta z \cos(\phi)}{\sum_{N_y} \sum_{N_x} \Delta z \cos(\phi)}, \quad (3)$$

where Δz is the geopotential height response at a given point, λ is longitude, ϕ is latitude, N_y the number of latitudes considered, and N_x the number of longitudinal grid points considered at a given latitude. Similarly, the response latitude ϕ_{NP} is computed as

$$\phi_{\text{NP}} = \frac{\sum_{N_y} \sum_{N_x} \phi \Delta z \cos(\phi)}{\sum_{N_y} \sum_{N_x} \Delta z \cos(\phi)}. \quad (4)$$

3 | RESULTS

3.1 | ENSO position and asymmetry

Figure 1 shows Pacific SST anomalies during El Niño and La Niña in HadISST, the HR multimodel ensemble and LR multimodel ensemble. Consistent with previous studies, positive SST anomalies associated with El Niño extend too far westward (around 20°) in LR models. However, this problem is alleviated in HR models, with the western

edge of positive SST anomalies closely matching that of HadISST. The difference in western extent between HR and LR models is highly significant: we find that all four LR models are further west than all eight HR models (not shown; see also Figure 2). Negative SSTs during La Niña also extend too far westward (by about 15°) in LR models. This issue is greatly reduced in HR models, and the difference between the two sets of models is again highly significant with no overlap.

To further investigate this improvement, Figure 2 shows equatorial SST anomalies during El Niño (a) and La Niña (b) over a 10° longitude region in the Pacific chosen so that the mean observed SST anomaly during the relevant ENSO phase is as close to zero as possible; these regions are 160–170°E for El Niño and 147–157°E for La Niña, and are shown in Figure 1. As well as HadISST and the HR and LR ensembles, we also split the HR ensemble into models where the atmospheric resolution at 0°N is less than 50 km (HR Atmos) and those where it is greater or equal to 50 km (LR Atmos; the atmospheric resolutions of these models are comparable to those of LR ocean models). From Figure 2a, it is clear that a strong positive SST anomaly (>0.7 K, approximately two-thirds of the average Niño 3.4 anomaly) remains on average in LR models in this region, whereas observed anomalies transition from negative to positive. On the other hand, only a small positive anomaly exists in the HR models, which is not significantly different to the observations. Figure 2b shows that negative SST anomalies in LR models during La Niña also extend into the region where observed anomalies transition to zero, with an average anomaly of around –0.5 K. HR models see significant improvement during La Niña, but the magnitude of the remaining anomaly is considerably larger than that for El Niño, and the difference between models and observations is significant above the 5% level.

For both El Niño and La Niña, the HR and LR atmosphere models within the HR ensemble are not significantly different to each other, despite the highly significant improvement seen when comparing HR and LR ocean models. This means that it is highly likely that the improvement in ENSO SST anomalies is due to the increase in ocean resolution, rather than through aliasing with increased atmospheric resolution.

The observed composite response to El Niño in Figure 1 shows a strong positive SST anomaly along the coast of Peru. This is largely associated with strong El Niño events and LR models fail to capture it, with SST anomalies only moderately higher than surrounding areas. HR models accurately capture the strength of this feature, although it should be noted that a similar (negative) response appears in the HR La Niña composite that is not present in observations or LR models. Overall, the spatial pattern of El

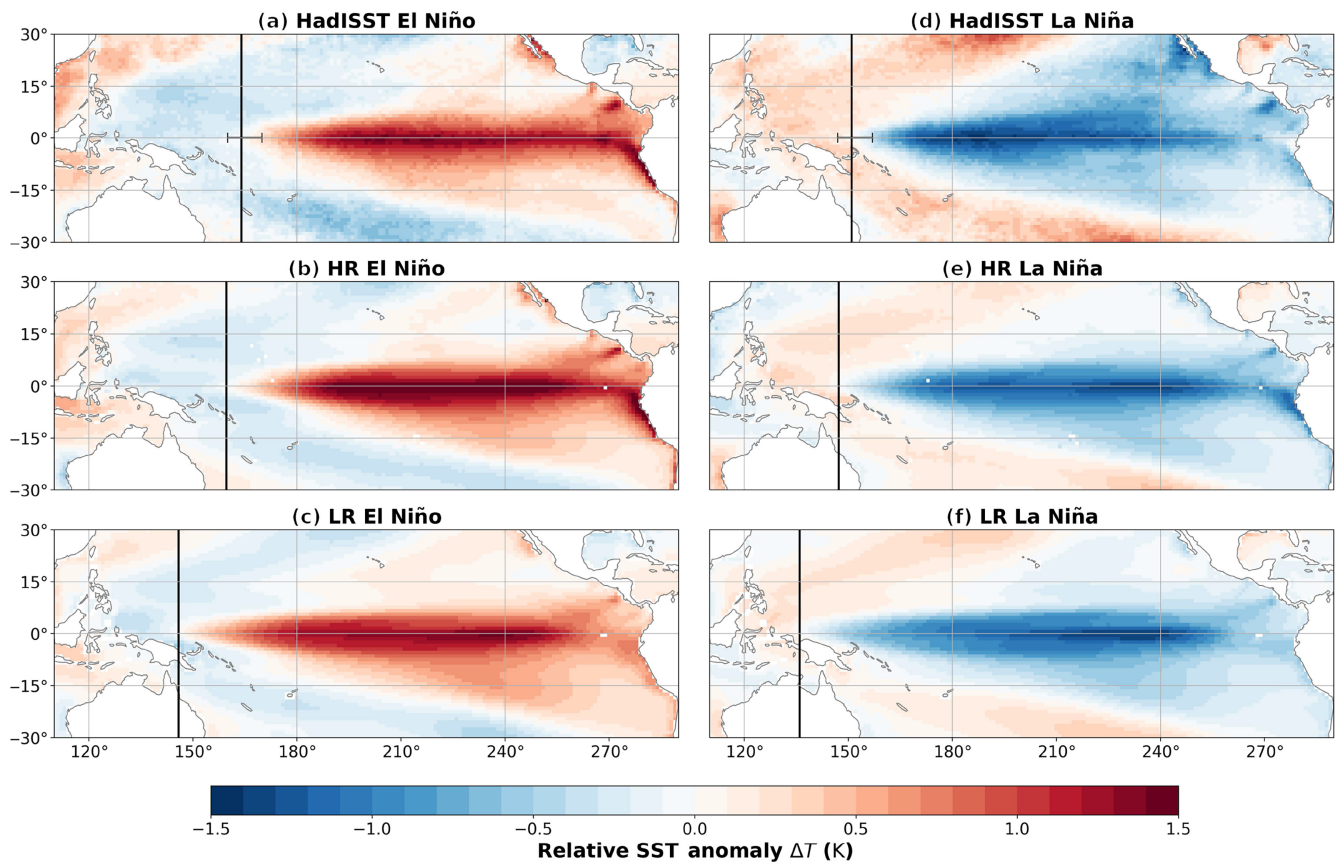


FIGURE 1 Sea-surface temperature (SST) patterns during El Niño and La Niña in observations and high-resolution (HR) and low-resolution (LR) models. SST anomaly during El Niño in (a) HadISST, (b) HR models, and (c) LR models (c), and during La Niña in (d) HadISST, (e) HR models, and (f) LR models. Vertical black lines represent where the SST anomaly changes sign on the Equator. Horizontal black lines on the Equator in (a) and (d) bound the regions used in Figure 2.

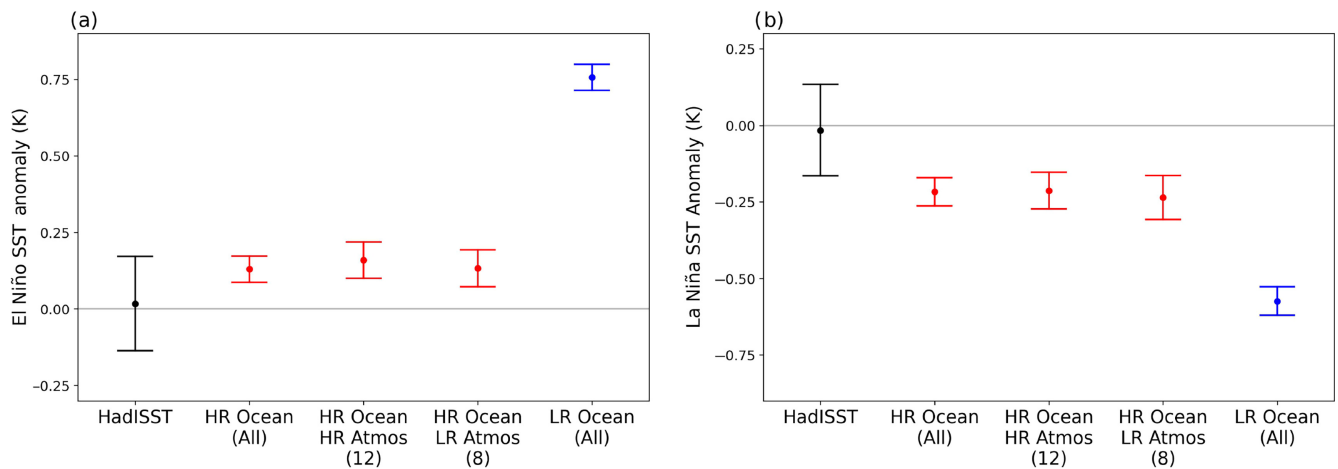


FIGURE 2 El Niño–Southern Oscillation sea-surface temperature (SST) anomalies where observed anomalies change sign. (a) Equatorial SST anomalies during El Niño, averaged over 160–170°E. (b) Equatorial SST anomalies during La Niña, averaged over 147–157°E. Each pane shows (left to right) HadISST, all high-resolution (HR) models, HR models with an atmospheric resolution at 0°N of less than 50 km, HR models with an atmospheric resolution at 0°N of greater or equal to 50 km, and all low-resolution (LR) models. Error bars deviate from the mean by the standard error multiplied by 1.96, to represent the 5%–95% confidence interval, with the standard error calculated using all individual realisations of El Niño or La Niña events.

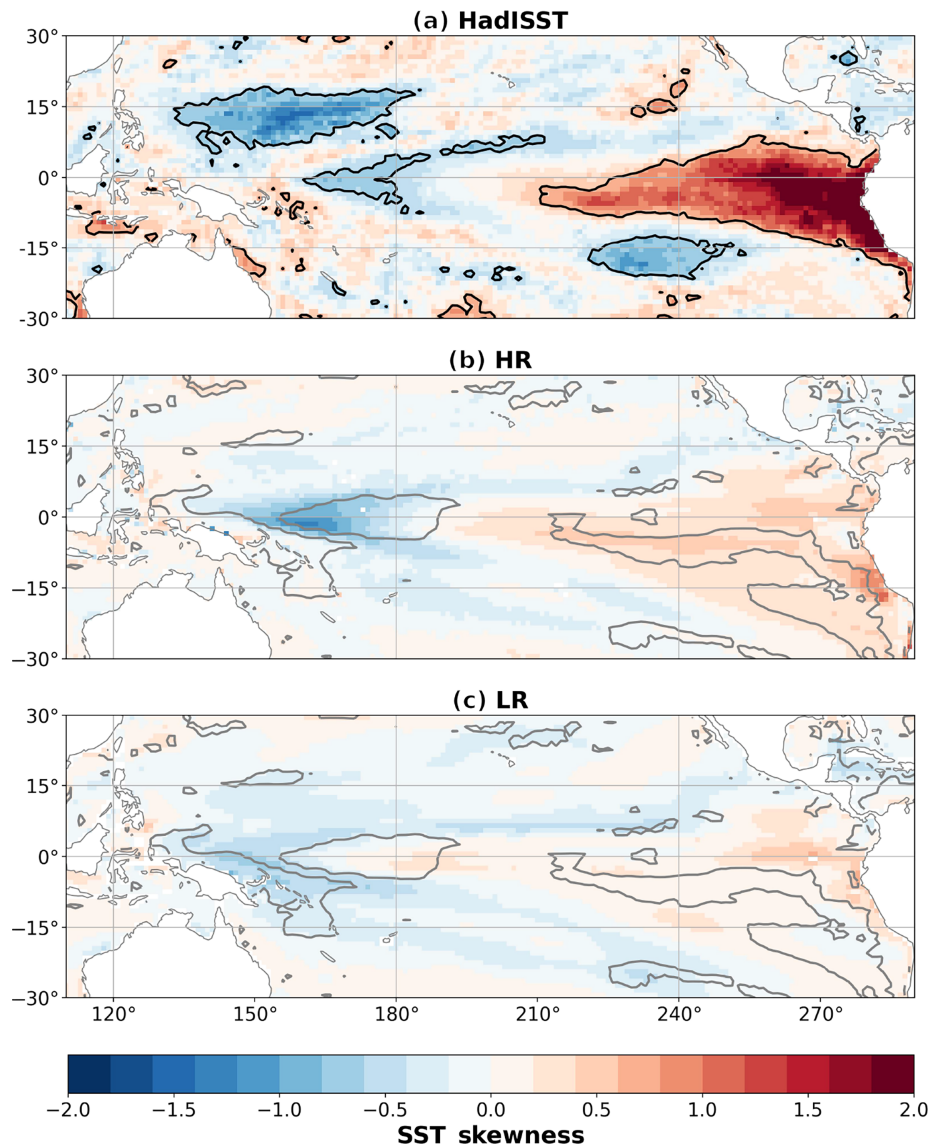


FIGURE 3 Sea-surface temperature (SST) asymmetry in observations and high- (HR) and low-resolution (LR) models. Skewness of interannual December–March SSTs in (a) HadISST, (b) HR models, and (c) LR models. Black contours in (a) enclose regions significant at the 5% level. Grey contours in (b) and (c) enclose regions where the skewness of the HR and LR ensembles are significantly different at the 5% level, computed using a two-sample *t* test on the skewnesses of individual ensemble members.

Niño and La Niña SST anomalies is greatly improved in HR models compared with LR models.

As explained in Section 1, climate models show a persistent problem with lack of ENSO asymmetry. Figure 3 shows the skewness of Pacific DJFM SSTs in HadISST, HR models, and LR models. Negative SST anomalies during La Niña extend further west in the tropical Pacific (see Figure 1) than positive SST anomalies during El Niño, leading to the negative skewness in the central-western tropical Pacific in Figure 3a. La Niña SST anomalies are also centred further west, resulting in positive skewness in the eastern tropical Pacific. Additionally, the ENSO response in the far east of the basin is highly nonlinear, with a relatively weak response except in the case of strong El Niño events—leading to the high positive skewness in Figure 3a. LR models strongly underestimate the asymmetry in the eastern Pacific, with skewness values that are only a small fraction of those observed. The negative-skew

ness in the western Pacific is more accurate, although shifted westward as expected from Figure 1. HR models still underestimate observed skewness in the eastern Pacific, but it is significantly improved in some regions, particularly away from the coast and south of the Equator. Additionally, negative skewness in the western tropical Pacific extends further east in HR models relative to LR, in line with observations.

3.2 | North Pacific teleconnection

Next, we consider the capability of HighResMIP models to represent teleconnections from El Niño and La Niña to the North Pacific. Figure 4 shows the response of 300 hPa geopotential height to El Niño and La Niña in the JRA-55 and HR and LR models. For El Niño, the central longitude λ_{NP} of the North Pacific response—characterised by

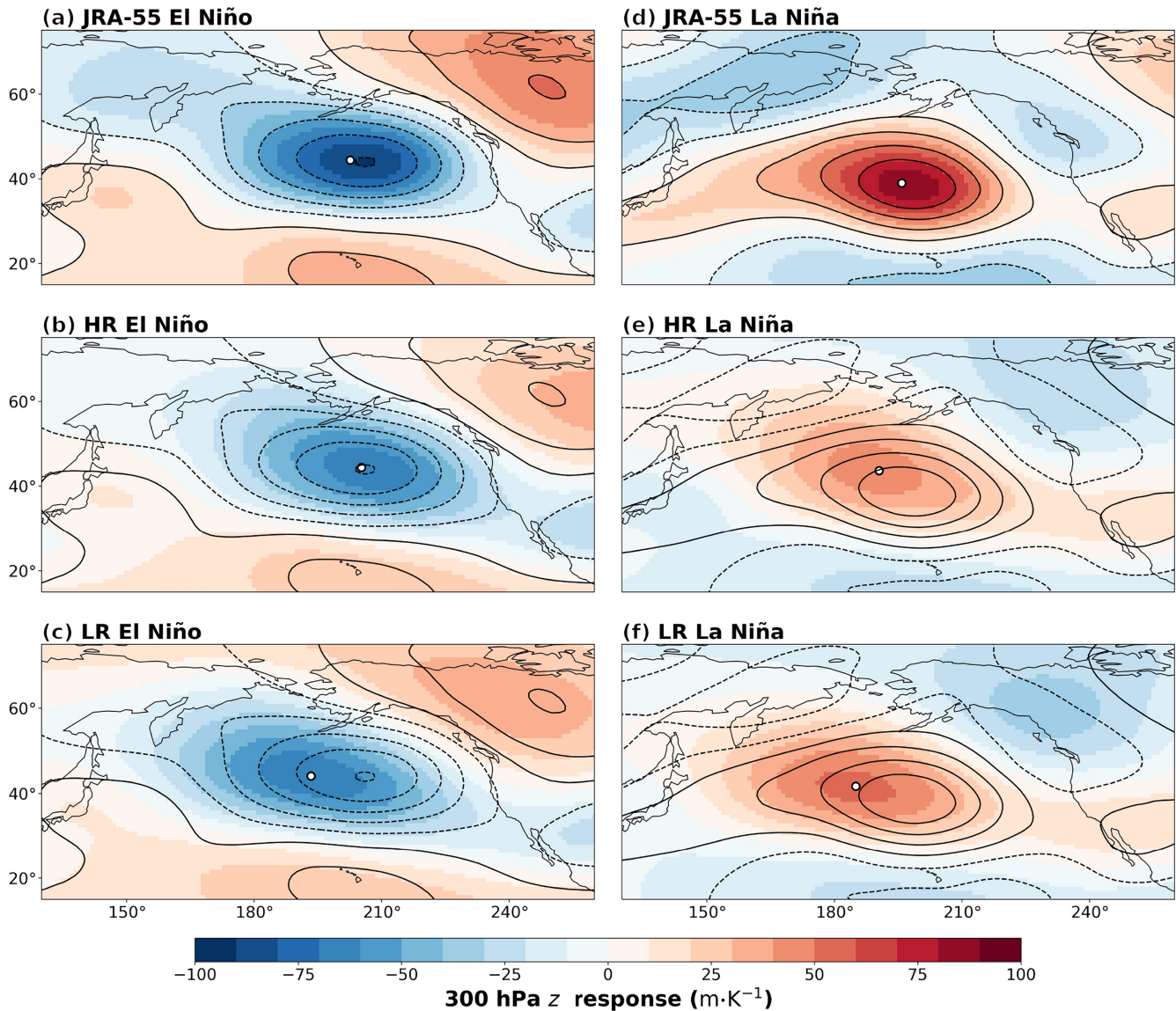


FIGURE 4 North Pacific geopotential height responses to El Niño–Southern Oscillation in observations and models. The 300 hPa geopotential height response divided by (absolute) Niño 3.4 anomaly during El Niño in (a) the Japanese 55-year Reanalysis (JRA-55), (b) high-resolution (HR) models, and (c) low-resolution (LR) models, and during La Niña in (d) JRA-55, (e) HR, and (f) LR. Black contours in (b), (c), (e), and (f) show the observed response in intervals of $20 \text{ m}\cdot\text{K}^{-1}$, from -90 to $+90 \text{ m}\cdot\text{K}^{-1}$. White circles mark the central longitude λ_{NP} and latitude ϕ_{NP} of the response.

a deepening of the climatological Aleutian low—behaves as expected given the zonal extent of tropical SST anomalies: the LR teleconnection is too far west, whereas the central longitude of the HR ensemble is very accurate. This demonstrates that the improvement in SST patterns shown in Figure 1 has translated into a corresponding improvement in the position of the teleconnection. The strength of the LR teleconnection during El Niño is weak by a factor of almost a half, which has previously been found to be the case in seasonal (Williams et al., 2023) and subseasonal (Garfinkel et al., 2022) forecasts. There is no discernible change in teleconnection amplitude with increased ocean resolution in the HR models.

Although there is significant improvement in the zonal position of the La Niña teleconnection with resolution, the HR teleconnection remains further west than the observed teleconnection. As with El Niño, both the LR and HR teleconnections are much weaker than observed. The HR teleconnection is slightly weaker than the LR teleconnection, but this is not significant. Both teleconnections are centred further north than observed: by around 3° for LR and 5° for HR. This has an impact on the location of teleconnection impacts around the North Pacific and further along the teleconnection chain towards Europe, and it also affects the strength of impacts, as winds in geostrophic balance scale inversely with the Coriolis parameter: in the

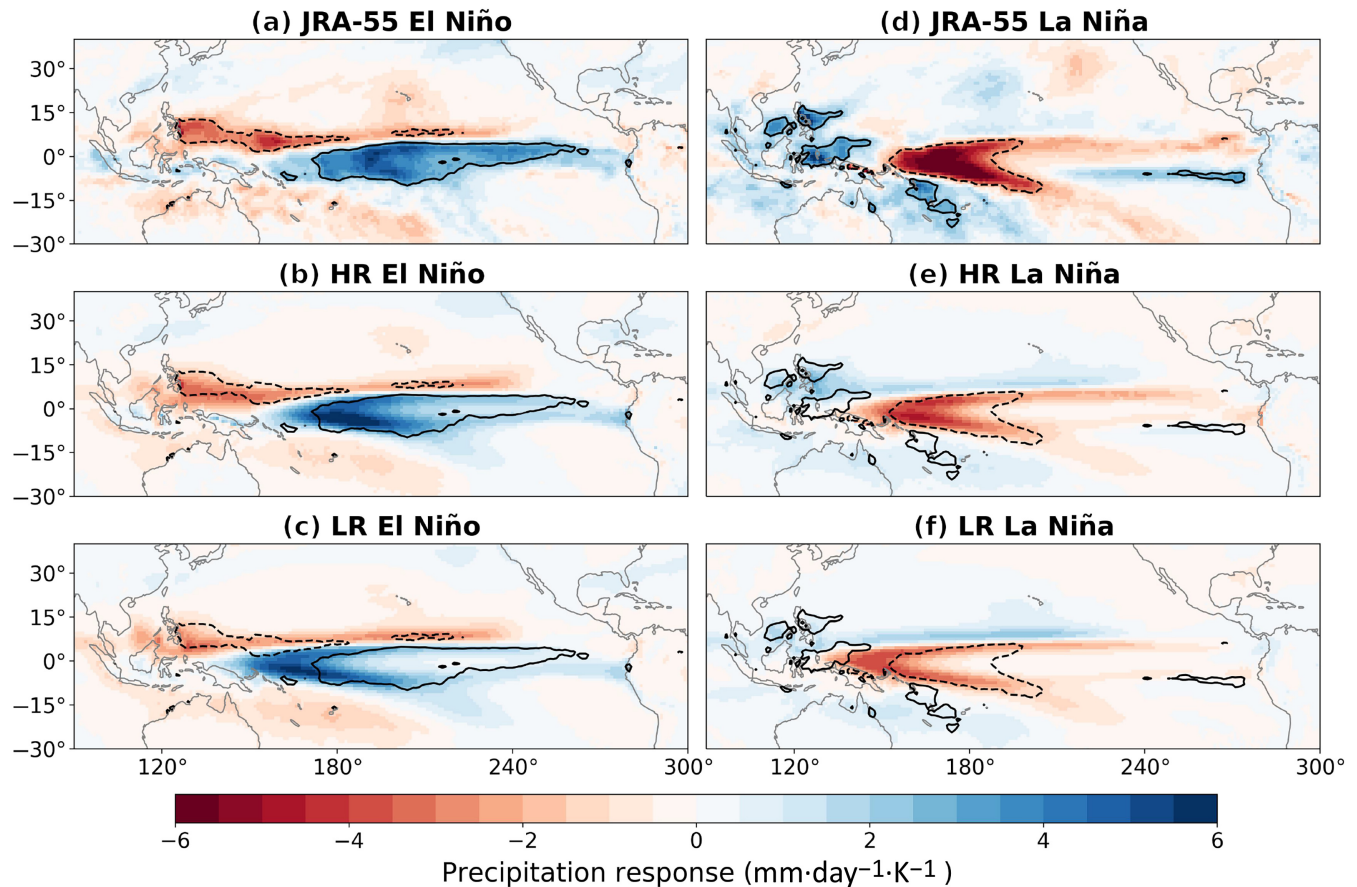


FIGURE 5 Changes in tropical precipitation during El Niño and La Niña. Precipitation response to El Niño per unit Niño 3.4 anomaly in (a) the Japanese 55-year Reanalysis (JRA-55), (b) HR models, and (c) LR models. Precipitation response to La Niña per unit Niño 3.4 anomaly in (d) JRA-55, (e) HR models, and (f) LR models. Black contours enclose regions where the JRA-55 precipitation response is less than $-3 \text{ mm}\cdot\text{day}^{-1}\cdot\text{K}^{-1}$ (dashed) or greater than $+3 \text{ mm}\cdot\text{day}^{-1}\cdot\text{K}^{-1}$ (solid).

case of HR, geostrophic winds will be about 7% weaker than expected from considering the strength of the geopotential height response alone. The central latitude of the El Niño teleconnection does not vary significantly between HR/LR models and observations. In the next section, we assess the simulation of processes involved in the generation of the El Niño and La Niña teleconnections in order to further understand the impact of increasing resolution on teleconnections to the North Pacific.

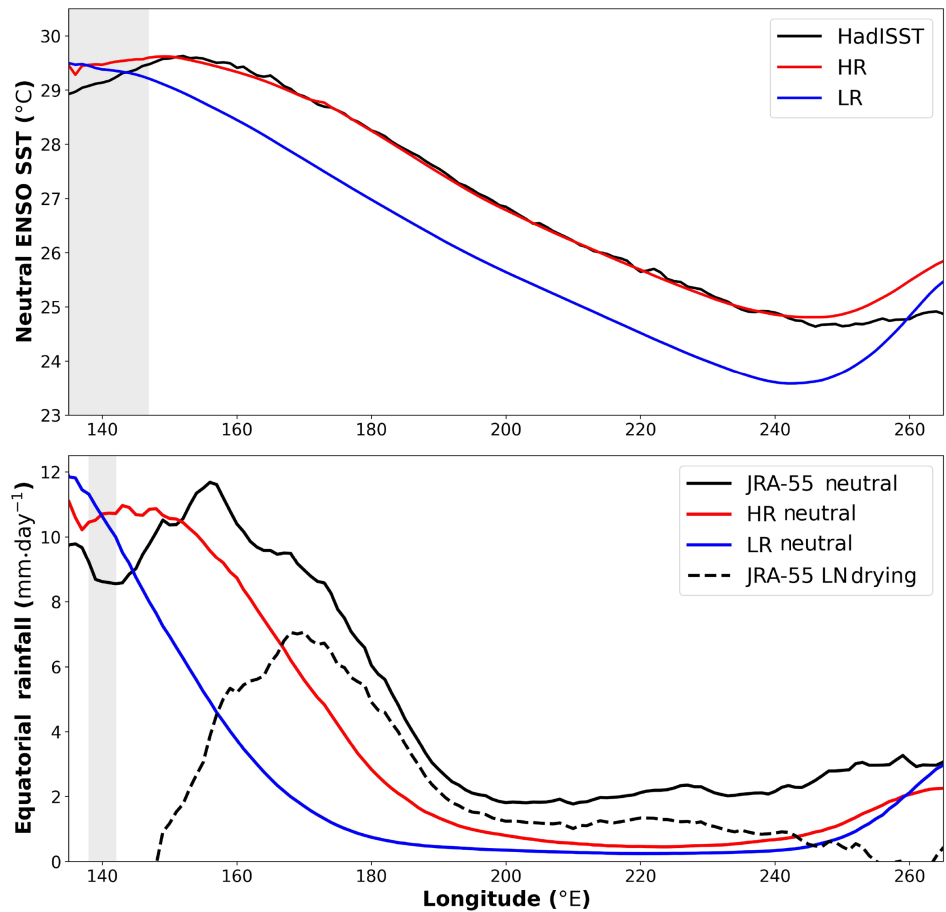
3.3 | Origin of teleconnection changes

Anomalous SSTs in the Tropics lead to anomalous precipitation, which is an important precursor to tropical-extratropical teleconnections. Figure 5a–c shows precipitation responses to El Niño in JRA-55 and HR and LR models. Consistent with SST anomalies, the positive precipitation response in the western-central Pacific extends further west in LR models than in HR models and JRA-55. Furthermore, in LR models, the precipitation response

is very weak over the region where the observed positive response is strongest (shown by solid black contours). In HR models, the precipitation is of comparable strength to that observed in this region. The difference between the LR and HR responses is consistent with the improvement in El Niño SSTs and the teleconnection to the North Pacific.

Figure 5d–f shows precipitation responses to La Niña in JRA-55 and HR and LR models. In the LR models, the drying response is strongest north of New Guinea, where the observed response transitions from negative to positive. The peak negative response is also smaller than observed. In the region where the observed drying response is strongest, the precipitation response in the LR models is very weak. The strongest drying response in the HR models is in a similar location to observed, but it is considerably weaker. Furthermore, the HR drying response extends further west than observed, despite the strong improvement in the western extent of SST anomalies. This is consistent with the weaker improvement in position for the North Pacific teleconnection during La Niña compared with El Niño.

FIGURE 6 Background sea surface temperatures (SSTs) and precipitation in the equatorial Pacific. (a) Neutral El Niño–Southern Oscillation (ENSO) SSTs on the Equator for Pacific longitudes, from HadISST (black) and high-resolution (HR; red) and low-resolution (LR; blue) models. (b) Neutral ENSO precipitation on the Equator for Pacific longitudes, from the Japanese 55-year Reanalysis (JRA-55; black solid) and HR (red) and LR (blue) models. The black dashed line in (b) shows the averaging drying response during La Niña (LN) according to JRA-55. Grey shading denotes where the difference between LR and HR is not significant at the 5% level, computed using a two-sided t test on the values for individual runs.



Both the anomalous and mean-state precipitation in the Tropics depend on the mean-state SSTs. Figure 6a shows mean-state (neutral) SSTs in the equatorial Pacific in HadISST and in HR and LR models. Away from the coast of South America, mean-state biases are largely eliminated in the central/eastern Pacific (around 170–260°E) in HR models, whereas the LR models are too cold by around 1°C. In the western Pacific (west of around 150°E) there is no real improvement with resolution and the two sets of models are not significantly different. We expect precipitation biases to reduce in line with the reduction in SST biases. Figure 6b shows the mean-state (neutral ENSO) precipitation in the equatorial Pacific in JRA-55 and in HR and LR models. Throughout most of the Pacific, HR and LR models both exhibit a dry bias, but with a smaller bias in HR models. Between 200 and 240°E, the mean-state precipitation in both sets of models is much closer to zero than observed. Mean-state precipitation in HR models starts to increase west of 200°E; this is consistent with observed mean-state precipitation, which exhibits similar behaviour, but there remains a significant dry bias in HR models until around 160°E. In LR models, precipitation remains close to zero until around 180°E, leading to a much larger bias than HR models between around 150 and 200°E.

The observed drying response during La Niña is shown by the dashed black line in Figure 6b. In this region, where it is strongest, both HR and LR models have a precipitation mean state that is less than the observed drying response. As a result, the observed response is physically impossible to realise in the models, leading to the weak precipitation responses to La Niña in models. Furthermore, the discrepancy between LR and HR precipitation mean states is largest in this region, leading to the very weak LR response to La Niña shown in Figure 5f. We find that the persistence of precipitation biases despite the removal of SST biases is due to weak sensitivity of precipitation to local SSTs (not shown), as has been found in previous studies (Good et al., 2021; Liu et al., 2022; Moreno-Chamarro et al., 2022).

4 | DISCUSSION AND CONCLUSIONS

Increasing ocean resolution from 1° to 0.25° in state-of-the-art climate models leads to meaningful reduction in several persistent and widespread errors relevant to ENSO simulation. The large error of the westward extension of El Niño and La Niña SST anomalies is largely eliminated. This improvement was previously reported

when comparing the standard and HR EC-Earth models in HighResMIP (Haarsma et al. 2020; using the standard deviation of tropical Pacific SSTs), and when comparing the LR and middle-resolution version of HadGEM3-GC3.1 (Menary et al. 2018; for El Niño only). By considering a larger set of models, we confirm the robustness of this result. In addition, the asymmetry between El Niño and La Niña is greatly improved. Improvements in the position and asymmetry of ENSO SST anomalies with increased resolution may be due to improved capability in resolving tropical instability waves (Graham, 2014). Nonlinear heat advection is important for ENSO asymmetry (Ineson et al., 2021) and may also improve with increased resolution. The position of the El Niño teleconnection to the North Pacific also improves. However, long-standing errors in tropical mean-state precipitation persist, leading to a teleconnection that only partly improves during La Niña. The improvement in teleconnection position is consistent with Dawson et al. (2013), who found similar results in an earlier version of the HadGEM model; their study varied ocean and atmospheric resolution independently and found that the improvement in teleconnection simulation was a result of increased ocean resolution.

State-of-the-art climate models have a high computational cost that scales quadratically with increased horizontal resolution; in practice, an increase in spatial resolution requires an increase in temporal resolution, leading to an even higher computational cost. By demonstrating that long-standing model errors (which may prove difficult to address by another method) are reduced or even eliminated by doing so, we show that increasing resolution is desirable. Nonetheless, the issue of underestimated North Pacific teleconnection strength remains, and persistent precipitation biases mean that the improvements in La Niña simulation do not lead to equivalent improvements in the teleconnection position.

Although this study focuses on late winter (JFM), we found that the errors in ENSO–North Pacific teleconnections, and how they change with resolution, are consistent when using December–February means instead (not shown). We include the 1/12° ocean HadGEM3-GC3.1-HH model with the 0.25° ocean models throughout this study; it was found to perform comparably to the other HR models in all areas we consider. It should be noted that ocean resolution is not the only way that the models differ—the tuning of the ocean model, the atmospheric model used, and the resolution of the atmospheric model are different in each model. Our focus on the means of all HR and all LR models helps to account for this. Atmospheric resolution is higher on average in HR models, but we show that there are no significant differences in ENSO SST anomalies from HR models with atmospheric resolutions similar to LR models and those

with a higher atmospheric resolution. We note that a different model set is used in the LR and HR composites. However, when we weight model centres equally (e.g., the five Met Office Hadley Centre model runs combined in HR are weighted equally to the single Centre National de Recherches Météorologiques run) and removing the Centro Euro-Mediterraneo sui Cambiamenti Climatici models, the results are qualitatively unchanged (not shown); this is also true if the Centro Euro-Mediterraneo sui Cambiamenti Climatici models are included. Therefore, we are confident that ocean resolution is the main driver of differences between the HR and LR ensembles.

This investigation demonstrates that increased ocean resolution in models has a major impact on the simulation of ENSO and associated teleconnections. We find major improvements in SST anomalies due to ENSO in the tropical western Pacific. This has a significant impact on simulated climate variability over the Maritime Continent. We show that this improvement leads to a more accurate teleconnection pattern in the North Pacific during El Niño and La Niña, which is important for modelling the climate of North America and further along the teleconnection pathway in Europe (e.g., Honda et al., 2001). The amplitude of the El Niño–North Pacific teleconnection is found to be weak in both the LR and HR models; this is relevant to the unresolved signal-to-noise paradox (Scaife & Smith, 2018), which arises due to models underestimating the predictable component of atmospheric variability. Finally, improved ENSO asymmetry in HR models may be helpful in simulating the nature and impact of strong El Niño events.

ACKNOWLEDGEMENTS

N.C.W. was supported by a Natural Environment Research Council (NERC) GW4+ Doctoral Research Partnership Studentship (NE/L002434/1). A.A.S. was supported by the Met Office Hadley Centre Climate Programme funded by BEIS.

DATA AVAILABILITY STATEMENT

The HighResMIP and HadISST data used in this study are freely available online at <https://esgf-index1.ceda.ac.uk/search/cmip6-ceda/> under the HighResMIP target MIP. The JRA-55 data used in this work are freely available at <https://doi.org/10.5065/D60G3H5B/>.

ORCID

Ned C. Williams  <https://orcid.org/0000-0002-0296-4271>

REFERENCES

- Ayarzagüena, B., Ineson, S., Dunstone, N.J., Baldwin, M.P. & Scaife, A.A. (2018) Intraseasonal effects of El Niño–southern oscillation on North Atlantic climate. *Journal of Climate*, 31, 8861–8873.

- Burgers, G. & Stephenson, D.B. (1999) The “normality” of El Niño. *Geophysical Research Letters*, 26, 1027–1030.
- Cagnazzo, C. & Manzini, E. (2009) Impact of the stratosphere on the winter tropospheric teleconnections between ENSO and the North Atlantic and European region. *Journal of Climate*, 22, 1223–1238.
- Cai, W., Santoso, A., Wang, G., Wu, L., Collins, M., Lengaigne, M. et al. (2020) ENSO response to greenhouse forcing. In: McPhaden, M.J., Santoso, A. & Cai, W. (Eds.) *El Niño southern oscillation in a changing climate*. New York: Wiley, pp. 289–307.
- Dawson, A., Matthews, A.J. & Stevens, D.P. (2011) Rossby wave dynamics of the North Pacific extra-tropical response to El Niño: importance of the basic state in coupled GCMs. *Climate Dynamics*, 37, 391–405.
- Dawson, A., Matthews, A.J., Stevens, D.P., Roberts, M.J. & Vidale, P.L. (2013) Importance of oceanic resolution and mean state on the extra-tropical response to El Niño in a matrix of coupled models. *Climate Dynamics*, 41, 1439–1452.
- Deser, C. & Wallace, J.M. (1987) El Niño events and their relation to the southern oscillation: 1925–1986. *Journal of Geophysical Research: Oceans*, 92, 14189–14196.
- Deser, C. & Wallace, J.M. (1990) Large-scale atmospheric circulation features of warm and cold episodes in the tropical Pacific. *Journal of Climate*, 3, 1254–1281.
- Garfinkel, C.I., Chen, W., Li, Y., Schwartz, C., Yadav, P. & Domeisen, D. (2022) The winter North Pacific teleconnection in response to ENSO and the MJO in operational subseasonal forecasting models is too weak. *Journal of Climate*, 35, 4413–4430.
- Good, P., Chadwick, R., Holloway, C.E., Kennedy, J., Lowe, J.A., Roehrig, R. et al. (2021) High sensitivity of tropical precipitation to local sea surface temperature. *Nature*, 589, 408–414.
- Graham, T. (2014) The importance of eddy permitting model resolution for simulation of the heat budget of tropical instability waves. *Ocean Modelling*, 79, 21–32.
- Haarsma, R., Acosta, M., Bakhshi, R., Bretonnière, P.-A., Caron, L.-P., Castrillo, M. et al. (2020) HighResMIP versions of EC-earth: EC-Earth3P and EC-Earth3P-HR—description, model computational performance and basic validation. *Geoscientific Model Development*, 13, 3507–3527.
- Haarsma, R.J., Roberts, M.J., Vidale, P.L., Senior, C.A., Bellucci, A., Bao, Q. et al. (2016) High resolution model intercomparison project (HighResMIP v1. 0) for CMIP6. *Geoscientific Model Development*, 9, 4185–4208.
- Hardiman, S.C., Dunstone, N.J., Scaife, A.A., Smith, D.M., Comer, R., Nie, Y. et al. (2022) Missing eddy feedback may explain weak signal-to-noise ratios in climate predictions. *npj Climate and Atmospheric Science*, 5, 57.
- Hayashi, M., Jin, F.-F. & Stuecker, M.F. (2020) Dynamics for El Niño-La Niña asymmetry constrain equatorial-pacific warming pattern. *Nature Communications*, 11, 4230.
- Honda, M., Nakamura, H., Ukita, J., Kousaka, I. & Takeuchi, K. (2001) Interannual seesaw between the Aleutian and Icelandic lows. Part I: seasonal dependence and life cycle. *Journal of Climate*, 14, 1029–1042.
- Horel, J.D. & Wallace, J.M. (1981) Planetary-scale atmospheric phenomena associated with the southern oscillation. *Monthly Weather Review*, 109, 813–829.
- Ineson, S., Dunstone, N.J., Ren, H.-L., Renshaw, R., Roberts, M.J., Scaife, A.A. et al. (2021) ENSO amplitude asymmetry in met Office Hadley Centre climate models. *Frontiers in Climate*, 3, 789869.
- Ineson, S. & Scaife, A.A. (2009) The role of the stratosphere in the European climate response to El Niño. *Nature Geoscience*, 2, 32–36.
- Kang, I.-S., Kug, J.-S., Lim, M.-J. & Choi, D.-H. (2011) Impact of transient eddies on extratropical seasonal-mean predictability in DEMETER models. *Climate Dynamics*, 37, 509–519.
- Kennedy, J., Titchner, H., Rayner, N. & Roberts, M. (2017) *input4MIPs. MOHC. SSTsAndSeaIce. HighResMIP. MOHC-HadISST-2-2-0-0-0. Version 20170505*. Earth System Grid Federation. 10. <https://esgf-node.llnl.gov/search/input4mips>
- Kobayashi, S., Ota, Y., Harada, Y., Ebata, A., Moriya, M., Onoda, H. et al. (2015) The JRA-55 reanalysis: general specifications and basic characteristics. *Journal of the Meteorological Society of Japan. Ser. II*, 93, 5–48. Available from: <https://doi.org/10.2151/jmsj.2015-001>
- Larkin, N.K. & Harrison, D. (2002) ENSO warm (El Niño) and cold (La Niña) event life cycles: ocean surface anomaly patterns, their symmetries, asymmetries, and implications. *Journal of Climate*, 15, 1118–1140.
- Li, G. & Xie, S.-P. (2014) Tropical biases in CMIP5 multimodel ensemble: the excessive equatorial Pacific cold tongue and double ITCZ problems. *Journal of Climate*, 27, 1765–1780.
- Li, R.K., Woollings, T., O’Reilly, C. & Scaife, A.A. (2020) Effect of the North Pacific tropospheric waveguide on the fidelity of model El Niño teleconnections. *Journal of Climate*, 33, 5223–5237.
- Li, T. (1997) Phase transition of the El Niño–southern oscillation: a stationary SST mode. *Journal of the Atmospheric Sciences*, 54, 2872–2887.
- Lin, J.-L. (2007) The double-ITCZ problem in IPCC AR4 coupled GCMs: ocean–atmosphere feedback analysis. *Journal of Climate*, 20, 4497–4525.
- Liu, B., Gan, B., Cai, W., Wu, L., Geng, T., Wang, H. et al. (2022) Will increasing climate model resolution be beneficial for ENSO simulation? *Geophysical Research Letters*, 49, e2021GL096932.
- Luo, J.-J., Masson, S., Roeckner, E., Madec, G. & Yamagata, T. (2005) Reducing climatology bias in an ocean–atmosphere CGCM with improved coupling physics. *Journal of Climate*, 18, 2344–2360.
- Madec, G., Bourdallé-Badie, R., Bouttier, P.-A., Bricaud, C., Bruciaferri, D., Calvert, D. et al. (2017) *NEMO ocean engine*. Note du Pôle de modélisation de l’Institut Pierre-Simon Laplace Technical report 27.
- Menary, M.B., Kuhlbrodt, T., Ridley, J., Andrews, M.B., Dimdore-Miles, O.B., Deshayes, J. et al. (2018) Preindustrial control simulations with HadGEM3-GC3. 1 for CMIP6. *Journal of Advances in Modeling Earth Systems*, 10, 3049–3075.
- Moreno-Chamarro, E., Caron, L.-P., Loosveldt Tomas, S., Vegas-Regidor, J., Gutjahr, O., Moine, M.-P. et al. (2022) Impact of increased resolution on long-standing biases in HighResMIP-PRIMAVERA climate models. *Geoscientific Model Development*, 15, 269–289.
- Moron, V. & Gouirand, I. (2003) Seasonal modulation of the El Niño–southern oscillation relationship with sea level pressure anomalies over the North Atlantic in October–March 1873–1996. *International Journal of Climatology: A Journal of the Royal Meteorological Society*, 23, 143–155.
- Okumura, Y.M. & Deser, C. (2010) Asymmetry in the duration of El Niño and La Niña. *Journal of Climate*, 23, 5826–5843.

- Rasmusson, E.M. & Carpenter, T.H. (1982) Variations in tropical sea surface temperature and surface wind fields associated with the southern oscillation/El Niño. *Monthly Weather Review*, 110, 354–384.
- Sardeshmukh, P.D. & Hoskins, B.J. (1988) The generation of global rotational flow by steady idealized tropical divergence. *Journal of the Atmospheric Sciences*, 45, 1228–1251.
- Scaife, A.A. & Smith, D.M. (2018) A signal-to-noise paradox in climate science. *npj Climate and Atmospheric Science*, 1, 1–8.
- Titchner, H.A. & Rayner, N.A. (2014) The met Office Hadley Centre sea ice and sea surface temperature data set, version 2: 1. Sea ice concentrations. *Journal of Geophysical Research: Atmospheres*, 119, 2864–2889.
- Toniazzo, T. & Scaife, A.A. (2006) The influence of ENSO on winter North Atlantic climate. *Geophysical Research Letters*, 33, L24704.
- Williams, N.C., Scaife, A.A. & Screen, J.A. (2023) Underpredicted ENSO teleconnections in seasonal forecasts. *Geophysical Research Letters*, 50, e2022GL101689.
- Zhang, T. & Sun, D.-Z. (2014) ENSO asymmetry in CMIP5 models. *Journal of Climate*, 27, 4070–4093.

How to cite this article: Williams, N.C., Scaife, A.A. & Screen, J.A. (2024) Effect of increased ocean resolution on model errors in El Niño–Southern Oscillation and its teleconnections. *Quarterly Journal of the Royal Meteorological Society*, 1–12. Available from: <https://doi.org/10.1002/qj.4655>